Changes in the Global Carbon Cycle and Ocean Circulation on the Millennial Time Scale

Thomas F. Stocker
Climate and Environmental Physics
Physics Institute, University of Bern
Sidlerstrasse 5, CH–3012 Bern, Switzerland
stocker@climate.unibe.ch

Global Climate, Museu de la Ciencia de Barcelona

February 2, 2001

Abstract

Carbon dioxide is, after water vapor, the most important greenhouse gas. Naturally, its atmospheric concentration has varied between 190 and 290 ppmv over the last half million years. The man-made CO_2 increase of the last 250 years has already reached this amplitude with the potential of inducing significant global warming. Climate models suggest that the ocean circulation reacts in a sensitive way to global warming in that large circulation systems can break down. Here we discuss the question of potential feedback mechanisms between the global carbon cycle and the ocean circulation. This is done by first examining the paleoclimatic record of past CO_2 changes obtained from polar ice cores. Modelling experiments provide a quantitative interpretation of the changes found in these records.

1 Introduction

Greenhouse gases play a crucial role in the energy balance of the Earth. In order to illustrate the importance of these gases, the simplest climate model is considered. Were the Earth a black body which is in thermal equilibrium with the incoming short wave radiation from the sun, the following energy balance can be formulated:

$$\pi R^2 \cdot (1-\alpha) \cdot S_0 = 4\pi R^2 \cdot \sigma \cdot T^4 \tag{1}$$

where $R = 6730\,\mathrm{km}$ is the Earth's radius, $\alpha = 0.3$ is the global mean albedo (reflectivity), $S_0 = 1367\,\mathrm{Wm^{-2}}$ is the solar constant, $\sigma = 5.67 \cdot 10^{-8}\,\mathrm{Wm^{-2}K^{-4}}$ is the Stefan-Boltzmann constant (Fig. 1). Solving for the global mean annual temperature, we obtain:

$$T = \left[\frac{(1-\alpha)\cdot S_0}{4\cdot\sigma}\right]^{0.25} = -18.3^{\circ}\mathrm{C}. \tag{2}$$

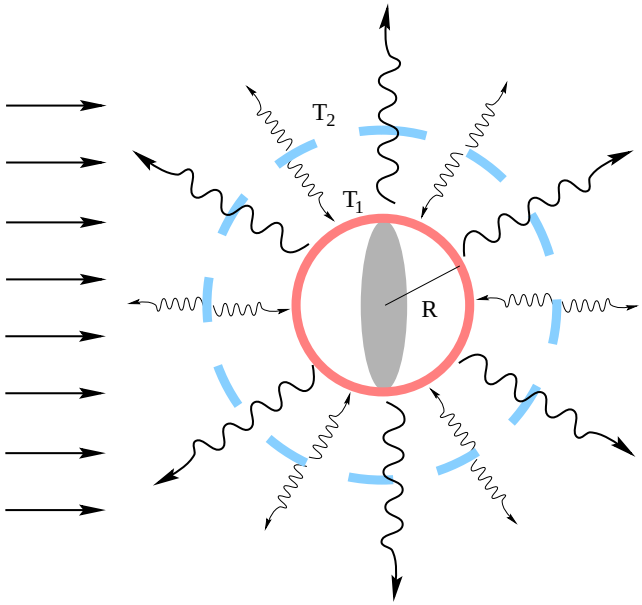

Figure 1: A minimum climate model in which the Earth is assumed to be a black body in radiative equilibrium with incoming solar short wave, outgoing longwave radiation at temperature T_1 and a layer at higher altitude ("clouds"), which emits radiation as a black body at temperature T_2.

This is in contrast with observations, and T is below the freezing point of water. Therefore life in its current form would not be possible. Instead, the mean annual temperature is about +15°C. An increase in surface temperature can be qualitatively obtained by introducing a second black-body shell at a higher altitude. This shell shall represent the combined effect of clouds, water vapor and other greenhouse gases and is assumed to be transparent to shortwave radiation and opaque to longwave radiation. We also assume that this shell is only partly present to mimic the effects of an incomplete "cloud" cover. This fraction is denoted by c. The energy balance for such a configuration then reads:

$$\pi R^2 \cdot (1-\alpha) \cdot S_0 + c \cdot 4\pi R^2 \cdot \sigma \cdot T_2^4 = 4\pi R^2 \cdot \sigma \cdot T_1^4, \tag{3}$$

$$c \cdot 4\pi R^2 \cdot \sigma \cdot T_1^4 = 2 \cdot c \cdot 4\pi R^2 \cdot \sigma \cdot T_2^4, \tag{4}$$

where T_1 and T_2 are now the temperatures of the surface and the outer shell, respectively. Note that in the above equations, the "cloud" cover does not change albedo; this is not correct for clouds at mid and low altitudes. Assuming a fractional "cloud" cover of 77%, the equilibrium temperatures are now:

$$T_1 = +14.6°\text{C}, \qquad \text{and} \qquad T_2 = -31.1°\text{C}. \tag{5}$$

Equivalently, one could argue that the greenhouse effect is taken into account by simply assuming that the Earth is a grey body with emissivity ϵ. This planetary emissivity is estimated at about $\epsilon = 0.6$ which yields an equilibrium temperature of

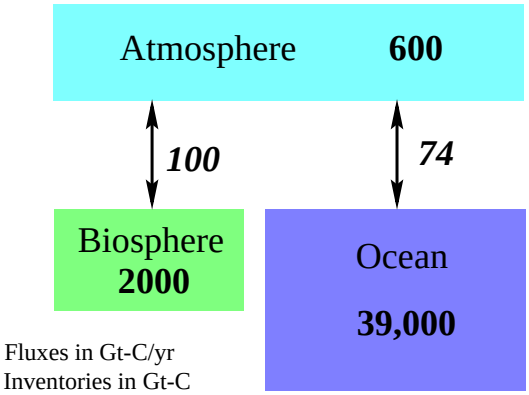

Figure 2: The global carbon cycle involves three fast exchanging reservoirs: the atmosphere, the ocean and the terrestrial biosphere. Carbon inventories and exchange fluxes are indicated. This is a simplified version of the figure by Siegenthaler & Sarmiento (1993).

$$T = \left[\frac{(1-\alpha)\cdot S_0}{4\cdot\epsilon\cdot\sigma}\right]^{0.25} = +16.4°\mathrm{C}. \tag{6}$$

What is parameterised here bluntly in the form of a 2-shell Earth or a simple "grey body" is in reality the cumulative effect of all radiatively active gases in the atmosphere. Their order of importance is water vapor, carbon dioxide (CO_2), methane (CH_4) and nitrous oxide (N_2O). It is thus of prime importance to document and understand past changes in these radiatively active agents in order to be able to estimate the effect of future changes in the radiative balance of the Earth.

Past changes in the content of the most important greenhouse gas, water vapor, cannot be directly reconstructed. Only indirect paleoclimatic evidence such as changes in snow-line elevation is available which might be employed to estimate changes in the vertical lapse rate and hence in the water vapor content. Further, stable isotopes of the water molecule ($\delta^{18}O$ and $\delta^{2}H$) determined on ice cores from different altitudes may provide additional information. The concentrations of the other greenhouse gases, however, can be reconstructed for the past by measuring air entrapped in polar ice cores (Raynaud *et al.* 1993).

2 Carbon Cycle

In order to understand changes in the global carbon cycle of the Earth due to anthropogenic activity during the last 250 years, the natural cycle is briefly revisited. For a comprehensive review the reader is referred to Siegenthaler & Sarmiento (1993). For time scales not exceeding a few thousand years, the most important reservoirs are the atmosphere, the ocean and the terrestrial biosphere (Fig. 2). Carbon appears in different forms in these reservoirs: in the atmosphere it is primarily CO_2, in the terrestrial biosphere in

the form of fixed carbon in organic matter, whereas in the ocean the major part of the inventory is in the form of the bicarbonate ion (HCO_3^-). The ocean inventory is over 60 times larger than the atmospheric inventory and about 20 times larger than the terrestrial biosphere inventory and is thus the most important component in determining the level of atmospheric CO_2. Carbon is naturally cycled through these three reservoirs, and the atmosphere serves as a gateway with a relatively short residence time of about $600/(100+74) \approx 3.5$ years. The exchange mechanisms between atmosphere and terrestrial biosphere are photosynthesis (uptake of CO_2 from the atmosphere) and respiration (release of CO_2 to the atmosphere), whereas gas exchange dominates the fluxes between the ocean and the atmosphere.

Carbonate chemistry in the surface waters of the ocean is central to the understanding of the influence of and dynamics of changes in the ocean carbon content upon atmospheric CO_2. Here we follow Joos & Sarmiento (1995). In the ocean surface waters, dissolved inorganic carbon occurs in the three species

$$[CO_2] : [HCO_3^-] : [CO_3^{2-}] = 1 : 175 : 21, \tag{7}$$

which implies that only a very small fraction of dissolved inorganic carbon (about 1%) can exchange with the atmosphere. The three species are in chemical equilibrium

$$CO_2 + CO_3^{2-} + H_2O \longleftrightarrow 2 \cdot HCO_3^-, \tag{8}$$

and thus

$$\frac{[HCO_3^-]^2}{[CO_2] \cdot [CO_3^{2-}]} = \text{constant} \tag{9}$$

Because of the dominance of the bicarbonate pool, (9) can be approximated by

$$[CO_2] \cdot [CO_3^{2-}] \approx \text{constant}. \tag{10}$$

An additional constraint is the conservation of charge. This is taken into account by considering alkalinity, which can be defined as the total excess positive charge of all the ions in solution. Again, considering only the most important ionic species, an approximation is given by

$$[HCO_3^-] + 2 \cdot [CO_3^{2-}] \approx \text{constant}. \tag{11}$$

With these approximations, we can calculate the ratio of the relative changes in CO_2 and total carbon in the ocean:

$$\zeta = \frac{\frac{d[CO_2]}{[CO_2]}}{\frac{d([HCO_3^-] + [CO_3^{2-}])}{[HCO_3^-] + [CO_3^{2-}]}} = \frac{[HCO_3^-] + [CO_3^{2-}]}{[CO_3^{2-}]} \approx \frac{175 + 21}{21} \approx 9.3, \tag{12}$$

where (10) and (11) have been used. ζ is the buffer factor or *Revelle Factor* which is central to the understanding of the effects of changes in the ocean carbon inventory on the atmospheric CO_2 concentration. ζ depends on the chemical composition of the sea water, its salinity and temperature and ranges from about 8 in equatorial to about 14 in high-latitude waters (Takahashi *et al.* 1993). Relative inventory changes in the atmosphere are about 10 times larger than the corresponding relative changes in the ocean. This simplified reasoning also explains how much of an initial carbon injection into the atmosphere will remain there (assuming no interaction with the carbonate sediments). Assume that the carbon inventory in atmosphere increases by a small fraction f. The mass of additional carbon in the atmosphere and ocean is then given, respectively, by $f \cdot I_A$ and $(f/\zeta) \cdot I_O$, where I_A and I_O are the inventories of atmosphere and ocean as given in Fig. 2. The fraction of carbon that remains in the atmosphere (airborne fraction) can be calculated according to

$$r = \frac{f \cdot I_A}{f \cdot I_A + (f/\zeta) \cdot I_O} = \frac{1}{1 + \frac{1}{\zeta} \cdot \frac{I_O}{I_A}} \approx 13\%. \tag{13}$$

So far, only the inorganic aspect of the marine carbon cycle was discussed. However, using the above relations one would obtain an atmospheric CO_2 concentration of about 670 ppmv (parts per million by volume) for the atmosphere in chemical equilibrium with an abiotic ocean. This is in strong contrast to current observations indicating about 370 ppmv, and reconstructions of pre-industrial CO_2 concentration of about 280 ppmv (Neftel *et al.* 1988; Indermühle *et al.* 1999).

Therefore, there must exist additional processes that keep the concentration of CO_2 in the surface ocean low. These are collectively referred to as oceanic carbon "pumps" (Volk & Hoffert 1985). There are three such pumps: (i) the solubility pump; (ii) the soft tissue, or organic matter pump; and (iii), the calcite pump, and they maintain a vertical gradient of total dissolved inorganic carbon (DIC) in the water column. The solubility pump is due to the fact that warmer waters are less soluble for CO_2, i.e. both cold deep and cold high-latitude surface waters are enriched in CO_2 relative to the main water masses of the "warmwater sphere". This leads to a reduction of DIC in the surface waters. The soft tissue pump is due to the DIC uptake during the formation of marine organisms. This organic matter is constantly exported to the deep ocean in particulate and dissolved form. This also tends to reduce the surface concentrations of DIC. The third pump operates in the opposite direction. When organic matter forms calcite shells ($CaCO_3$), CO_3^{2-}-ions are extracted from the water column. Due to (10) this results in an increase of atmospheric CO_2. In combination, these three pumps lead to a reduction of the equilibrium CO_2-concentration in the atmosphere from 670 ppmv to 280 ppmv (Tab. 1).

solubility	organic matter	calcite	atm. CO_2
–	–	–	665 ppmv
√	–	–	380 ppmv
√	√	–	250 ppmv
√	√	√	**278 ppmv**

Table 1: The effect of the three carbon pumps calculated using the carbon cycle model of Joos *et al.* (1999) [calculations courtesy G.-K. Plattner, alkalinity held constant].

3 Ocean and Abrupt Climate Change

3.1 Climatically Relevant Ocean Circulation Types

The climate system consists of four major components. These are the atmosphere, the cryosphere, the terrestrial biosphere and the ocean. This subdivision is somewhat arbitrary and other approaches, e.g. according to the relevant cycles of heat, water and tracers, are equally valid. The terrestrial biosphere and the cryosphere (ice sheets) are important drivers of climate change. The former has a strong influence on the hydrological cycle and the albedo (Crowley & Baum 1997) whereas the ice sheets are mainly influencing atmospheric circulation and the surface radiative balance through the ice-albedo feedback (see Crowley & North 1991). For example, glacial-interglacial temperature reduction is not feasible without a strong contribution of land-surface changes. This is illustrated by taking the logarithmic derivative of (6):

$$\frac{\Delta T}{T} = \frac{1}{4} \cdot \frac{\Delta S_0}{S_0} - \frac{1}{4} \cdot \frac{\Delta \alpha}{1-\alpha} - \frac{1}{4} \cdot \frac{\Delta \epsilon}{\epsilon}. \tag{14}$$

Using estimates for the reduction of global mean annual temperature ($\Delta T \approx -4\,\mathrm{K}$), and solar radiation due to changes in orbital parameters ($\Delta S_0 \approx 0.3\,\mathrm{Wm}^{-2}$) during the last glacial maximum (Berger *et al.* 1993), we note from (14), that changes in solar forcing cannot explain directly the colder climate.

In addition, a strong ice-albedo feedback is required. This can be estimated in the following way. Albedo at 60°N is 0.4 in summer and about 0.55 in winter due to snow and sea ice cover (Peixoto & Oort 1992). The regions polewards of 60° account for about 6% of the surface area, therefore $\Delta\alpha \approx 0.06 \cdot 0.15$. Thus,

$$\frac{-4}{298} = \frac{0.3}{4 \cdot 1367} - \frac{0.01}{4 \cdot 0.5} - \ldots \tag{15}$$

demonstrates that albedo changes have the correct order of magnitude to change global mean temperature significantly. Such albedo changes are slow, because terrestrial ice sheets take several 10,000 years to build up. Rapid changes, which are abundantly found in the paleoclimatic record (e.g. Broecker 1997 for a review) cannot be explained by these processes alone.

Here, the ocean plays an important role. The ocean is a major important component of the climate system because it covers 70% of the Earth's surface. Considering ocean and

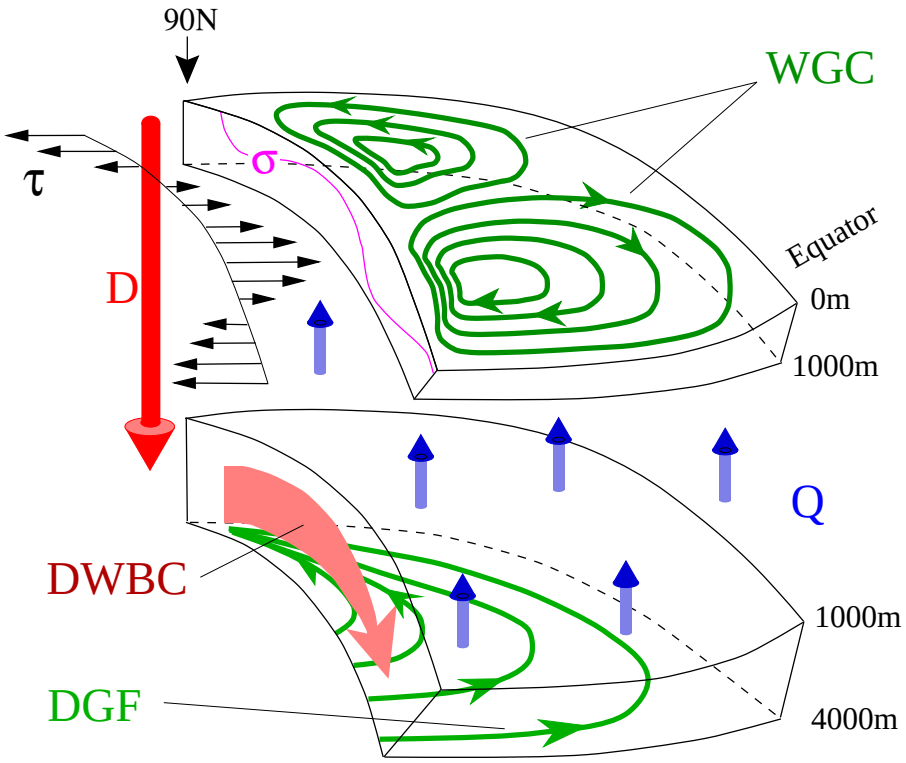

Figure 3: Schematic view of the different types of steady-state circulations in a sectorial ocean basin extending from the equator to the pole with a longitudinal extent of roughly 60°. Wind stress τ drives a *wind driven gyre circulation* (WGC) which shows western intensification due to the curvature of the rotating Earth. τ also causes Ekman upwelling in the northerly and Ekman downwelling in the southerly upper layer giving a near-surface isopycnal surface σ its typical shape: the isopycnal is shallow below the subpolar gyre and deep below the subtropical gyre. A source of newly formed deep water, D, feeds the deep ocean in which a *deep western boundary current* (DWBC) develops from which the *deep geostrophic flow* (DGF) of the interior is derived. DGF flows northward to conserve potential vorticity while slowly upwelling. This results in a vertical mass flux Q that closes the flow. In reality, $Q < D$ in this sector and the DWBC is crossing the equator setting up a global circulation [from Stocker 1999].

atmosphere as the only components that are relevant for climate changes on time scales of less than 10^4 years, the ocean contains 95% of water and 99.9% of the heat content. However, it is the dynamics that is essential in providing a mechanism for abrupt change.

The present description of ocean circulation types is very basic and concerns only the most important, large-scale flows; here we follow Stocker (1999). The major processes that govern the dynamics are the action and regional distribution of momentum and buoyancy fluxes at the ocean's surface, the Earth's rotation and the presence of ocean basin boundaries. Four major circulation types characterize the flow in an ocean basin on large spatial scales (Fig. 3). The general circulation is forced by the input of momentum through surface wind stress τ and by the flux of buoyancy, indicated by the vertical arrow D and uniform upwelling Q (Fig. 3). The surface wind stress forces the wind-driven geostrophic circulation (WGC) which is intensified at the western boundary and forms the subtropical and the subpolar gyres. In the interior of the ocean basin, there is a

balance between the pressure gradients and the Coriolis forces acting on the moving fluid. Western intensification, on the other hand, is a consequence of the spherical shape of the rotating Earth and frictional effects in the fluid and at the basin boundaries (Stommel 1948; Pedlosky 1996).

Winds blowing over the surface of the ocean lead to divergent (Ekman upwelling) or convergent (Ekman downwelling), frictionally driven flows and change the local depth of the near-surface isopycnals σ (lines of constant density) which set up horizontal pressure gradients with associated geostrophic flows. These flows are responsible for the fact that the wind driven gyres do not extend all the way to the bottom but are compensated by sloping isopycnals in the top few hundred meters. In other words, the geostrophic velocities exhibit a vertical structure and the wind-driven circulation remains confined to the top few hundred meters of the water column (Pedlosky 1996).

Turning now to the deep circulation, the source D feeds the deep western boundary current (DWBC) which flows southward and leaks into the deep interior where the geostrophic flow (DGF) is directed polewards at all latitudes. The DGF recirculates into the source area of the DWBC. There is a cross-interface mass flux Q upwelling into the upper 1000 m which supplies the mass lost due to D in the upper layer.

There are only a few locations in the ocean where new deep water is being formed. These are the Greenland-Iceland-Norwegian Seas in the north and the Weddell Sea in the south and a few other, minor sites (Killworth 1983; Marshall & Schott 1999). The dynamics of a fluid moving on a rotating sphere dictates that also the deep flow is confined to western boundary currents (Stommel 1958; Stommel & Arons 1960). In the present ocean, the northern source is strong enough so that the current crosses the equator and penetrates eventually into the southern ocean. There, it mixes with the deep waters from the Weddell Sea and flows into the Indian and Pacific oceans where broad upwelling occurs. The global structure of the deep water paths was already suggested by Henry Stommel (1920–1992) in a pioneering paper (Stommel 1958); the return flow in the thermocline, preferentially via the 'warm water route' around Africa, was first described by Gordon (1986). This global flow subsequently became known as the 'conveyor belt' (Broecker 1987; Broecker 1991), but the structure is far more complicated than a simple ribbon spanning the globe (Schmitz 1995).

Evaluations of the radiation balance at the top of the atmosphere show that the ocean-atmosphere system must transport heat towards the high latitudes where there is a net loss of energy over one year (Trenberth & Solomon 1994). About half of that heat is carried by ocean currents (Macdonald & Wunsch 1996). In contrast to the other ocean basins, the meridional heat transport in the Atlantic Ocean is northward at all latitudes. Evaluation of oceanographic observations (Hall & Bryden 1982) as well as model simulations (Böning *et al.* 1996) indicate that the meridional heat transport in the Atlantic is primarily due to the meridional overturning circulation which carries warm near-surface waters northward and cold deep water southward. This is the deep circulation of the ocean that is driven by surface buoyancy fluxes and is referred to as the "thermohaline circulation", short THC (Warren 1981). The wind-driven, near-surface circulations in the Atlantic do not transport significant amounts of heat polewards. The thermohaline circulation in the Atlantic is also often referred to as the "nordic heat pump".

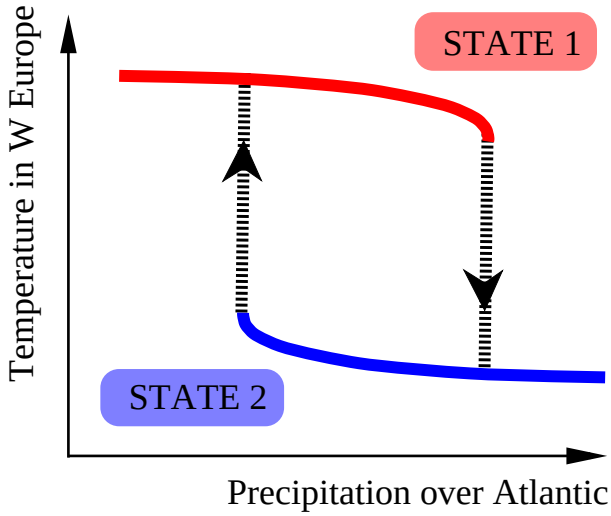

Figure 4: The ocean-atmosphere system is a non-linear physical system that can exhibit hysteresis behaviour of the deep circulation in the ocean (Stocker & Wright 1991). Depending on the surface freshwater balance of the Atlantic ocean, the meridional heat flux in the Atlantic is not unique and multiple equilibria exist. Changes are linear as long as they remain on the same branch of the hysteresis loop. If certain threshold values in the atmosphere-ocean system are passed, the climate state can change abruptly by switching from one branch to the other. This is a robust feature of the climate system as demonstrated by the entire hierarchy of climate models [from Stocker & Wright 1991].

The idea that the ocean has more than just a regulating or damping effect on climate changes goes back to Chamberlin (1906) who hypothesised that a reversal of the abyssal circulation could explain "some of the strange climatic phenomena of the past". Much later Stommel (1961) found two stable equilibrium states in a simple box model of the THC, and Bryan (1986) showed multiple equilibria of the THC in a 3-dimensional ocean model. This finally convinced researchers that the ocean takes a central and *active* role in the climate system.

F. Bryan also identified a positive feedback mechanism that maintains deep water formation at high latitudes. Surface waters that are transported by the WGC towards the sinking regions (Fig. 3) transport salt so that, when cooled down by atmosphere-ocean heat exchange, they loose sufficient buoyancy and sink. This mechanism operates in the northern North Atlantic but not in the North Pacific, where the water does not contain enough salt to become sufficiently dense. If now, for some reason, the flow of the dense water is diverted, cut off or even sufficiently diluted, the deep water formation can be reduced or even stopped. The THC then settles into a new state in which the meridional transport of heat is significantly reduced. Lower sea surface temperatures and cooling of the overlying air follows. Such different states could be realized in 2-dimensional thermohaline models (Marotzke *et al.* 1988; Wright & Stocker 1991; Stocker & Wright 1991), multi-basin 3-dimensional ocean models (Bryan 1986; Marotzke & Willebrand 1991; Mikolajewicz & Maier-Reimer 1994; Hughes & Weaver 1994; Rahmstorf & Willebrand 1995) and coupled atmosphere-ocean models (Manabe & Stouffer 1988; Schiller *et al.* 1997; Fanning & Weaver 1997).

All these models essentially exhibit a universal hysteresis behaviour (Fig. 4). This is

due to the non-linear processes that govern the atmosphere-ocean fluxes of buoyancy which are the drivers for the THC (Stocker & Wright 1991). Anomalies of sea surface temperature are removed rather efficiently by anomalies in the atmosphere-ocean heat flux because of the strong correlation between these two quantities. On the other hand, sea surface salinity anomalies are not correlated with anomalies in the net surface freshwater fluxes (evaporation–precipitation–runoff). Therefore, there is a large difference between the response time of these different anomalies (Rooth 1982). The important result of hysteretic behaviour is that certain perturbations in the climate system can induce abrupt, non-linear and sometimes irreversible reorganisations in the atmosphere-ocean system (Stocker 2000).

3.2 The Paleoclimatic Record

Abrupt warmings and gradual coolings with amplitudes of up to 10–15°C in Central Greenland (Severinghaus *et al.* 1998; Lang *et al.* 1999) characterized the glacial climate: about 23 of these, now referred to as Dansgaard/Oeschger (D/O) events, were found in the Greenland ice cores (Dansgaard *et al.* 1993), and in marine sediments (Bond *et al.* 1992; Bond & Lotti 1995; Hughen *et al.* 1996). Terrestrial records (Grimm *et al.* 1993) from the northern hemisphere show similar changes. While such climate signals appear wide-spread at least in the northern hemisphere, they are muted or absent in most records of the southern hemisphere. All D/O events exhibit a striking similarity in their temporal evolution: cooling extends generally over many centuries to about 3 kyr, while warming is abrupt and occurs within years or decades. This suggests that one common mechanism may be responsible for these climate swings. The recurrence time for the shorter D/O events is of the order of 1000 years.

Layers with abundant coarse-grain lithic fragments are found in marine sediments (Heinrich 1988), later termed "Heinrich Events", or short H-event (Broecker *et al.* 1992). They are thought to be detrital material transported from the bedrock underlying the great ice sheets to the North Atlantic by calving icebergs. This occurred through surging ice streams which then melted and provided an additional sediment layer. Mineralogical analysis of these layers reveal that their origin is the Canadian shield (Bond *et al.* 1992), but discharge can also be traced to the Fennoscandian (Fronval *et al.* 1995) and British ice sheets (McCabe & Clark 1998). Most of the debris material, however, originates from north of Hudson Bay (Gwiazda *et al.* 1996). The typical recurrence time is estimated at about 7 kyr, thus significantly longer than that for the D/O events found in the ice cores.

At first glance, D/O and H-events seem unrelated. However, Bond & Lotti (1995) shows in a high-resolution marine sediment core from the North Atlantic that smaller layers of ice rafted debris were buried between the prominent Heinrich layers, i.e. such layers also occur during or before D/O events. This is strong indication of a common cause or trigger in the climate system responsible for these changes. The different thickness of the debris layers for D/O and H events suggests that the response of the atmosphere-ocean system depends on the magnitude of the iceberg discharge and possibly involves threshold effects.

The two "fat" D/O events (number 8 and 12, 36 kyr and 45 kyr BP, respectively) are not only distinct by their duration, but they both occur after a H-event; other, shorter D/O

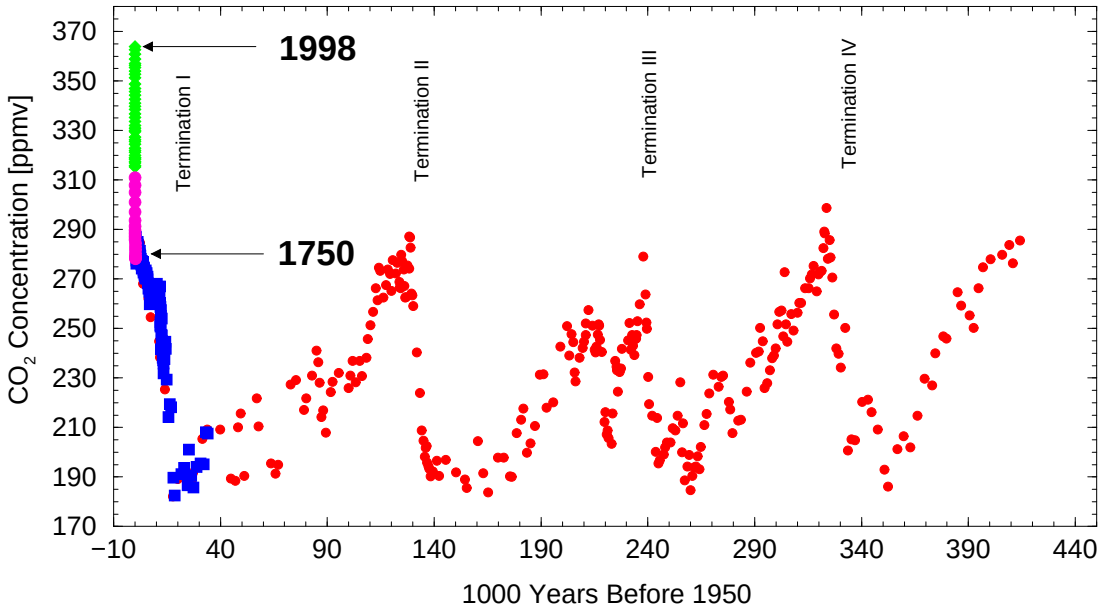

Figure 5: Complete composite CO_2 record over the last 420,000 years including 4 glacial cycles from direct measurements (Keeling & Whorf 1994, green diamonds), and ice core measurements from Siple Station (Neftel *et al.* 1985, magenta squares), Taylor Dome (Indermühle *et al.* 1999, Fischer *et al.* 1999, blue squares), and Vostok Station (Petit *et al.* 1999, red dots).

events do not have a preceeding H event. They are clearly associated with climate change derived from the isotopic changes in the Antarctic ice cores (Blunier *et al.* 1998). The warming in the Antarctic record appears steady over about 2 kyr and leads the abrupt warming recorded in the Greenland ice core. At the time of the northern warming, the Antarctic signal indicates a gradual return to colder temperatures over the next 2 kyr. Interestingly, these are also the two times when a clear increase in CO_2 of about 20 ppmv is detected (see below). Recent measurements confirm this finding and suggest two further events of Antarctic warming around 50 and 58 kyr BP which may be connected to rapid change in the north (Indermühle *et al.* 2000).

The above paleoclimatic evidence is consistent with and supports the hypothesis that the ocean plays the major role in causing the abrupt changes and transmitting the related signals. In particular, a collapse of the THC would stop the nordic heat pump leading to a severe cooling in the northern North Atlantic region. As the once active pump has been drawing heat from the southern ocean (Crowley 1992), this heat is now slowly accumulating in the southern ocean leading to warming. The climate system thus appears to operate as a bipolar seesaw during abrupt climate change (Broecker 1998; Stocker 1998).

4 Reconstructed Changes in Atmospheric CO_2

4.1 Evidence from Polar Ice Cores

Polar ice cores permit the reconstruction of past CO_2 concentrations over at least 4 glacial cycles (Petit *et al.* 1999). Prior to the formation of ice, accumulated snow is sintering into firn, a porous material which is in contact with atmospheric air (Schwander *et al.*

1997). Upon closure of the air-filled spaces in the firn, the composition of the air remains trapped in the bubbles within the ice matrix. Provided no further physical fractionation processes or chemical reactions occur, the air remains conserved in the bubbles. It depends on the location and the content of trace materials (dust, organic matter) whether these conditions are sufficiently satisfied. Once the ice core is retrieved from the ice sheets, the air is analyzed with various methods to provide information on past concentration of trace gases in ancient air (Raynaud *et al.* 1993). Carbon dioxide concentration is measured using a laser absorption technique and recent applications are described by Stauffer *et al.* (1998) and Indermühle *et al.* (1999).

For the other greenhouse gases, different analysis methods are applied. Methane is measured using gas chromatography (Blunier *et al.* 1998), the same technique also allows the determination of past concentrations of N_2O (Flückiger *et al.* 1999). In contrast to the vast majority of paleoclimatic data, CO_2, CH_4 and N_2O are among the very few variables that can be determined directly. Because they are not proxy data, one does not have to determine transfer functions or use modern analogue assumptions which may not be valid (Johnsen *et al.* 1995). Further direct data are isotopic and elemental concentrations of the gases trapped in the bubbles (e.g. O_2/N_2, $\delta^{15}N$).

Fig. 5 shows the most recent and complete reconstruction of past CO_2 changes. Atmospheric CO_2 concentrations vary in concert with the cycles of glaciation being around 270 to 290 ppmv during warm phases (interglacials) and around 190 ppmv during full glacial times. The continuous rise over the last 250 years is clearly unprecedented. Never in the last 420,000 years was the atmospheric CO_2 concentration as high as it is now (Petit *et al.* 1999). Calculations and various lines of independent evidence confirm that the recent rise, which by now is as large as the natural glacial-interglacial amplitude of CO_2, is due to the emission of CO_2 from fossil fuel burning and land use changes. Calculations which also take into account the changes of the isotopes of CO_2 (^{13}C and ^{14}C) permit the distinction of changes in the carbon inventories of the atmosphere, ocean and the terrestrial biosphere (Joos *et al.* 1999).

High-resolution CO_2 measurements by Stauffer *et al.* (1998), Indermühle *et al.* (1999), and Fischer *et al.* (1999) on Antarctic ice cores reveal a clearer picture of the dynamics of the global carbon cycle on time scales of less than a few 1000 years (Fig. 6). The variability of atmospheric CO_2 during the glacial does not exceed 20 ppmv, although a series of abrupt climate changes is evident in many paleoclimatic records (Broecker 1997). Some of these (the major Heinrich events and, associated with them, the longest of the Dansgaard/Oeschger events) are thought to be due to large atmosphere-ocean reorganizations in the form of complete collapses of the Atlantic THC (Stocker 2000). In order to test such hypotheses with physical-biogeochemical climate models, the measured amplitude and timing of the CO_2 changes serve as crucial constraints.

Another unexpected secular change in atmospheric CO_2 was the increase during the Holocene (the last 10 kyr) which is a relatively stable climate period (Indermühle *et al.* 1999). Major atmosphere-ocean reorganizations are absent with the possible exception of the brief cooling at 8200 kyr BP (Alley *et al.* 1997). Changes of the order of 20 ppmv can thus also occur naturally *without* large changes in ocean circulation.

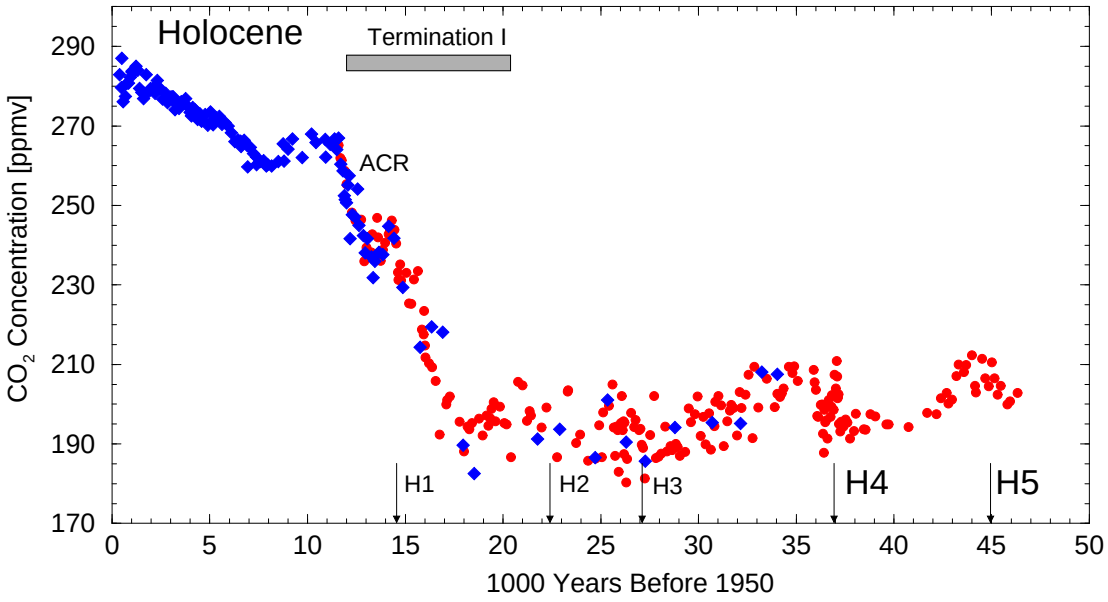

Figure 6: High-resolution CO_2 record from Byrd (Stauffer *et al.* 1998, red dots) and Taylor Dome (Indermühle *et al.* 1999, Fischer *et al.* 1999, blue diamonds) ice cores. The timing of Heinrich events (Broecker *et al.* 1992) is indicated by arrows. Those events in larger letters are associated with long D/O events found in Greenland ice cores (Dansgaard *et al.* 1993) and corresponding smaller climate changes in Antarctica (Blunier *et al.* 1998).

4.2 Possible Mechanisms for Atmospheric CO_2 Changes

Three types of CO_2 changes can be distinguished in Fig. 5 and Fig. 6:

1. glacial-interglacial changes of about 80 ppmv on time scales of about 10,000 years;
2. changes of about 20 ppmv on millennial time scale during the glacial, correlated with climatic changes;
3. changes of about 20 ppmv on millennial time scale during the Holocene.

It is a challenge of paleoclimatic and biogeochemical modeling to understand and quantitatively simulate these changes. There has been much progress over the last few years but some important aspects that are seen in the paleoclimatic records are not yet understood.

The longest-standing and still unresolved problem concerns the largest changes in the atmospheric CO_2 concentration, the glacial-interglacial changes. There have been a number of hypotheses explaining both the timing and the amplitude of the 80 ppmv changes but none of them is consistent with all available paleoclimatic evidence. A recent overview is given by Broecker & Henderson (1998) (their Tab. 1). None of the physical mechanisms such as changes in deep water circulation, cooler sea surface temperatures, or longer residence time of the waters in high northern latitudes can explain individually the amplitude of the CO_2 drop during the glacial (Siegenthaler & Wenk 1984). Furthermore, all scenarios using sea level rise as a driver (shelf inundation and shallow-water carbonate, coral-reef hypotheses) are not consistent because sea level rise occurs after the CO_2-increase. Finally, there is no clear paleoceanographic evidence for a significant increase in marine

productivity drawing down atmospheric CO_2; some of the stable isotope data, $\delta^{13}C$ in marine sediments, actually point to the contrary. Iron fertilization is another hypothesis. In some areas of the ocean, iron is a limiting nutrient and stronger dust input into the ocean by winds in a dustier atmosphere may enhance marine productivity resulting in lower atmospheric CO_2 (Martin 1990; Behrenfeld *et al.* 1996). As ice cores from Greenland and Antarctica indicate, the dust deposition drops significantly during the end of the glacial. However, the time scales of the changes in the dust supply are on the order of decades whereas those of CO_2 changes are millennia. At present, the most promising mechanisms appear to be linked to nutrient (through iron fertilization) and temperature changes in the Southern Ocean, with the nitrogen cycle playing an important role in explaining the relatively long time scales of CO_2 change. (Broecker & Henderson 1998).

High-resolution measurements in ice cores indicate that millennial changes of CO_2 during the glacial are less than about 20 ppmv (Stauffer *et al.* 1998; Indermühle *et al.* 2000). While earlier suggestions that CO_2, much like CH_4, would change during each D/O event could not be confirmed, the CO_2 changes appear correlated to (at least some) Heinrich events and/or the longest and most prominent of the D/O events (Fig. 6). About 2 kyr before the rapid warming seen in Greenland ice cores, CO_2 appears to rise. This rise coincides with a rise in temperature as indicated by the stable isotopes measured on Antarctic ice cores (Blunier *et al.* 1998; Indermühle *et al.* 2000), although there is still some uncertainty in the ice-age/gas-age difference. CO_2 therefore seems to be more closely linked with the climate changes in the south, than those in the north. How then, could one explain the warming in the south? Marine sediments contain layers of ice rafted debris at or before each D/O event (Bond & Lotti 1995). This suggests the presence of pools of freshwater which could have acted as triggers of changes in the THC of the Atlantic. Indeed, meltwater discharge to the North Atlantic would be the mechanism to explain the southern warming, because a cooling in the north, caused by the disruption of the nordic heat pump, would lead to a warming in the south. This strong north-south coupling appears to be present during the few H-events and subsequent "fat" D/O events but not during the shorter D/O events (Stocker 2000).

In order to test the hypothesis of strong north-south coupling during a complete collapse of the Atlantic THC, a simplified physical-biogeochemical climate model was used (Marchal *et al.* 1998). The discharge of a defined amount of freshwater into the North Atlantic disrupts the THC and lead to a collapse of the circulation. The strong cooling induced in the North Atlantic is compensated by a warming in the southern ocean through the effect of the "bipolar seesaw" (Broecker 1998; Stocker 1998). The cooling in the north would lead to an increased uptake of CO_2 through a stronger solubility pump, while the opposite is true for the southern ocean. While the global effect of changes in sea surface temperature remains less than about 5 ppmv with the warming in the south dominating the cooling in the North Atlantic, the combined effect of changes in DIC and alkalinity due to the discharge of the freshwater is an increase of atmospheric CO_2 a few 100 years after the full collapse of the THC in the North Atlantic. The net effect is thus an increase in atmospheric CO_2 between 7 and 30 ppmv on a timescale of 100 to 2000 years depending on the intensity of the THC change. At the time of abrupt warming in the north (resumption of the circulation), CO_2 is decreasing again. This is in qualitative agreement with the information from the ice cores. A recent study of the Younger Dryas confirms these findings (Marchal *et al.* 1999). Hence, the model suggests that the millennial CO_2 changes

are linked with ocean-atmosphere reorganizations triggered by freshwater pulses. It is important to note that the "chicken-and-egg" problem is not yet solved: did changes in the south trigger collapses of the Atlantic THC, or did ice sheet disintegration in the north trigger changes in ocean circulation? It is very likely that the sequence of H- and D/O events is a truly coupled ice-ocean-atmosphere phenomenon.

Changes of atmospheric CO_2 during the Holocene came as a surprise (Indermühle *et al.* 1999). It was long thought that the relatively stable climate period of the Holocene would also be reflected in the concentration of greenhouse gases. However, CH_4 showed a pronounced minimum at around 5 kyr BP indicating a weaker hydrological cycle in the low latitudes during that time (Blunier *et al.* 1995). Also CO_2 is not constant the Holocene but rises slowly by about 20 ppmv from about 8 kyr BP to the preindustrial level of 280 ppmv (Fig. 6). Here, ocean-atmosphere reorganizations cannot be invoked because rapid coolings and warmings, unlike during the glacial, have not occurred in this time period. Although sparse, data from the stable carbon isotope (^{13}C) of atmospheric CO_2 and model calculations indicate that most of the atmospheric carbon inventory increase comes from the terrestrial biosphere; a minor part would be due to a slow increase in global mean sea surface temperature during several thousand years. This highlights the importance of the terrestrial biosphere for millennial time scale changes of atmospheric CO_2. In consequence, more data of $^{13}CO_2$ are needed from polar ice cores.

5 Future Changes and Feedback Processes

It has been shown that the surface freshwater balance exerts a strong control on the THC in the North Atlantic (Manabe & Stouffer 1988; Stocker & Wright 1991; Mikolajewicz & Maier-Reimer 1994) and that multiple equilibria can result (Fig. 4). Warmer air temperatures, such as projected for the next century due to a continuing emission of greenhouse gases, are likely to enhance the hydrological cycle. This link between temperature and hydrological cycle is exhibited in the methane changes during each D/O event: the warming is associated with a 50% increase in the CH_4 concentration (Chappellaz *et al.* 1993). Warming would tend to strengthen evaporation at low latitudes, increase precipitation at higher latitudes and thus accelerate the hydrological cycle. As ocean models indicate, this would lead to a reduction of deep water formation in the northern North Atlantic due to a freshening of the surface waters. A reduction of sea surface density is also caused by the increased surface air temperatures further reducing the thermohaline circulation. While the relative strength of these two mechanisms is under debate (Dixon *et al.* 1999), a general reduction of the Atlantic THC in response to global warming appears to be a robust result found by the entire hierarchy of climate models (Manabe & Stouffer 1993; Manabe & Stouffer 1994; Stocker & Schmittner 1997; Wood *et al.* 1999).

As already Fig. 4 suggests, threshold values of key climate variables exist beyond which the THC can no longer be sustained. Among these are the level of greenhouse gases in the atmosphere (Manabe & Stouffer 1993) as well as the rate of increase of greenhouse gas concentration (Stocker & Schmittner 1997). The few model simulations show, that the critical level is somewhere between double and fourfold preindustrial CO_2 concentration, but this depends critically on various model parameterizations (Schmittner &

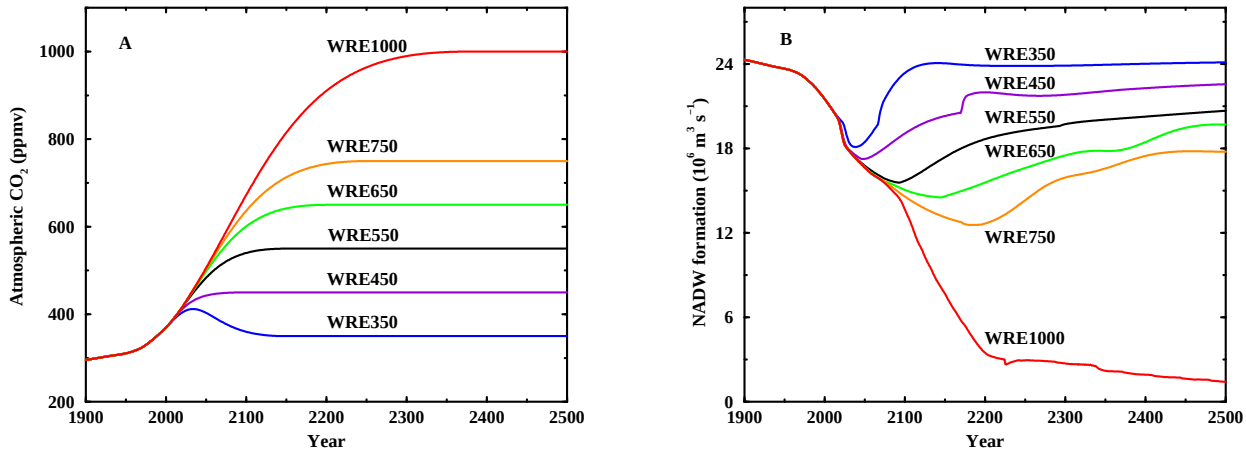

Figure 7: (A) Scenarios for the stabilization of atmospheric CO_2 concentration over the next 500 years; (B) evolution of the overturning circulation in the Atlantic in response to global warming caused by increasing concentration of CO_2. The climate sensitivity of the current experiments is 3.7°C for a doubling of CO_2 [From Joos *et al.* 1999].

Stocker 1999; Knutti *et al.* 2000). The threshold lies lower if the CO_2 increase is faster. If the threshold is crossed, a complete collapse of the Atlantic THC ensues which results in regional cooling and water mass reorganization very similar to the paleoclimatic experiments with the same model.

Model simulations using 3-dimensional ocean general circulation models with prescribed boundary conditions predicted a minor (Maier-Reimer *et al.* 1996) or a rather strong (Sarmiento & Le Quéré 1996) feedback between the circulation changes and the uptake of anthropogenic CO_2 under global warming scenarios. However, the complete interplay of the relevant climate system components was only taken into account in the recent study by Joos *et al.* (1999). A series of CO_2 stabilization profiles were prescribed for the next 500 years along with a specific climate sensitivity, i.e. the global mean temperature increase due to a doubling of CO_2: typically 1.5–4.5°C (Fig. 7a). As expected this leads to a reduction of the Atlantic THC. Again, a threshold value is between 750 and 1000 ppmv for a complete cessation of the THC (Fig. 7b).

With this model different experiments with the ocean carbon pumps operating or suppressed can be performed. Such experiments are essential for a better understanding of the various processes influencing ocean uptake of CO_2. A maximum uptake of 5.5 Gt/yr is simulated if there is no change in ocean circulation nor sea surface temperature. The full simulation including all feedbacks (sea surface temperature, circulation and biota) shows a long-term reduction of almost 50% in the uptake flux provided the Atlantic THC collapses (Fig. 8a). The solubility effect is important in the first 100 years (curve C) but later, the circulation effect takes over (curve D). If the circulation does not break down, circulation and biota feedback compensate each other, and the solubility effect remains the only significant feedback effect (Fig. 8b). The reduction of strength of the ocean as a major carbon sink appears a robust result, but the model also shows that dramatic feedback effects (such as a runaway greenhouse effect) are very unlikely. The

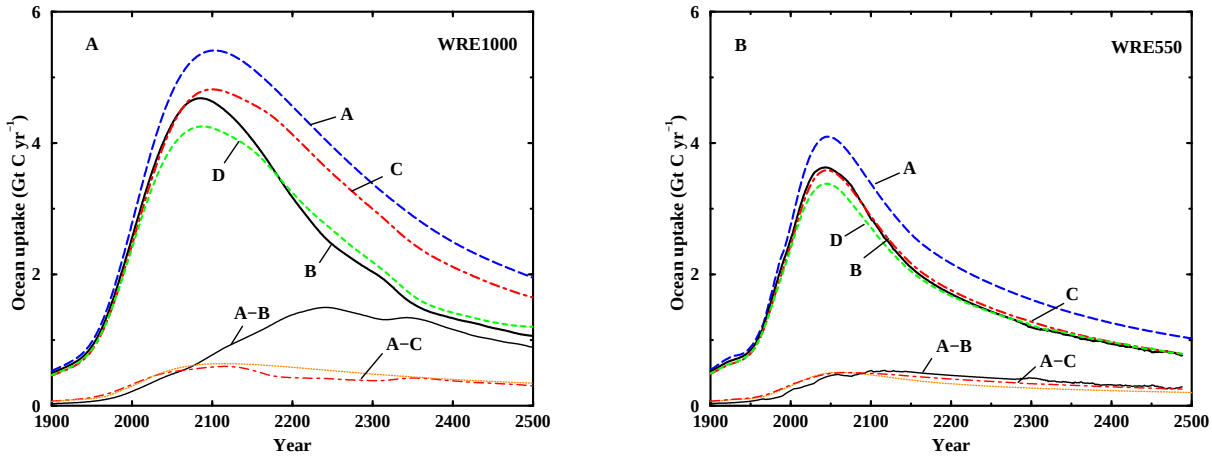

Figure 8: Evolution of the oceanic uptake of carbon dioxide for the different stabilization scenarios of Fig. 7. In WRE1000 (A), the Atlantic thermohaline circulation collapses completely by year 2500, in WRE500 (B) it remains close to the initial strength. The different simulations are labelled A–D. In A, all feedbacks are neglected (constant ocean), B is the full simulation (temperature, circulation, biota changes), C is only sea surface temperature changes (circulation held constant), D (temperature and circulation changes). Further explanations on regarding the different scenarios are in the text [From Joos *et al.* 1999].

maximum increase of CO_2 in the case of a collapsed Atlantic THC is estimated at about 20%. This result is entirely consistent with the evidence from the paleoclimatic records: major atmosphere-ocean reorganizations such as during H- or D/O-events appeared to have a relatively small influence on atmospheric CO_2.

6 Conclusions

The physical-biogeochemical state of the ocean is strongly influencing the atmospheric concentration of CO_2, the most important greenhouse gas after water vapor. The paleoclimatic record exhibits three different types of CO_2-changes, two of which are strongly associated with ocean circulation changes. By far the largest changes are the glacial-interglacial cycles of about 80 ppmv which still defy a complete, quantitative explanation. While the ocean plays a significant role through variations in the carbon pump strengths, most probably only a combination of different effects can explain the reconstructed changes. These include changes in the sea surface temperature, marine productivity, nitrogen fixation and in the interaction with carbonate sediments.

Two types of smaller CO_2-changes of the order of 20 ppmv have emerged from high-resolution measurements in Antarctic ice cores. The first appear to be correlated to the largest climate changes during the glacial, the H-events or the long D/O events of the Greenland ice cores. These climate changes are distinguished by the fact that changes in opposite phase are recorded in the Antarctic cores. This suggests an interhemispheric seesaw which is in operation during abrupt climate change. Simulations with coupled physical-biogeochemical climate models lend support to such a scenario. The driving

force is afforded by meltwater discharges from the northern hemisphere ice sheets which disrupt the Atlantic THC. CO_2 changes of similar magnitude also occur during relatively stable climate periods such as the Holocene. Here, changes are most likely due to a terrestrial biosphere which is still responding to the recent glacial-interglacial transition and continues to be influenced by changes in the hydrological cycle, land surface conditions (retreating ice cover) and climate.

The paleoclimatic record teaches us two lessons. First, future changes can only be understood if the full range of natural climate variability is reconstructed. Such reconstructions are crucial for a sensible climate model building and development. It is the past changes, free of anthropogenic perturbations, which these models must be capable of simulating. Second, by correlating climate changes documented in various archives with the ice core-based reconstructions of atmospheric CO_2, the link between the global carbon cycle and the atmosphere-ocean-biosphere system can be quantified. Model simulations suggest, that there is a potential in large non-linear changes in the physical climate system. These are shown to have an influence on the carbon cycle, on the uptake capacity of the world ocean and ultimately on the atmospheric concentration of CO_2.

Acknowledgment: I thank La Caixa for organising a stimulating conference in Barcelona. Comments by A. Indermühle, O. Marchal and G.-K. Plattner are appreciated. Financial support of the Swiss National Science Foundation and the Swiss Priority Program of Environment is acknowledged.

References

Alley, R. B., P. A. Mayewski, T. Sowers, M. Stuiver, K. C. Taylor, & P. U. Clark (1997). Holocene climatic instability: A prominent, widespread event 8200 yr ago. *Geology 25*, 483–486.

Behrenfeld, M. J., A. J. Bale, Z. S. Kolber, J. Aiken, & P. G. Falkowski (1996). Confirmation of iron limitation of phytoplankton photosynthesis in the equatorial Pacific Ocean. *Nature 383*, 508–511.

Berger, A., M.-F. Loutre, & C. Tricot (1993). Insolation and Earth's orbital periods. *J. Geophys. Res. 98*, 10341–10362.

Blunier, T., J. Chappellaz, J. Schwander, A. Dällenbach, B. Stauffer, T. F. Stocker, D. Raynaud, J. Jouzel, H. B. Clausen, C. U. Hammer, & S. J. Johnsen (1998). Asynchrony of Antarctic and Greenland climate change during the last glacial period. *Nature 394*, 739–743.

Blunier, T., J. Chappellaz, J. Schwander, B. Stauffer, & D. Raynaud (1995). Variations in the atmospheric methane concentration during the Holocene. *Nature 374*, 46–49.

Bond, G., H. Heinrich, W. Broecker, L. Labeyrie, J. McManus, J. Andrews, S. Huon, R. Jantschik, S. Clasen, C. Simet, K. Tedesco, M. Klas, G. Bonani, & S. Ivy (1992). Evidence for massive discharges of icebergs into the North Atlantic ocean during the last glacial period. *Nature 360*, 245–249.

Bond, G. C. & R. Lotti (1995). Iceberg discharges into the North Atlantic on millennial time scales during the last glaciation. *Science 267*, 1005–1010.

Böning, C., F. O. Bryan, W. R. Holland, & R. Döscher (1996). Deep-water formation and meridional overturning in a high-resolution model of the North Atlantic. *J. Phys. Oceanogr. 26*, 1142–1164.

Broecker, W. S. (1987). The biggest chill. *Natural Hist. 96*, 74–82.

Broecker, W. S. (1991). The great ocean conveyor. *Oceanography 4*, 79–89.

Broecker, W. S. (1997). Thermohaline circulation, the Achilles heel of our climate system: will man-made CO_2 upset the current balance? *Science 278*, 1582–1588.

Broecker, W. S. (1998). Paleocean circulation during the last deglaciation: a bipolar seesaw? *Paleoceanogr. 13*, 119–121.

Broecker, W. S., G. Bond, M. Klas, E. Clark, & J. McManus (1992). Origin of the northern Atlantic's Heinrich events. *Clim. Dyn. 6*, 265–273.

Broecker, W. S. & G. M. Henderson (1998). The sequence of events surrounding Termination II and their implications for the cause of glacial-interglacial CO_2 changes. *Paleoceanogr. 13*, 352–364.

Bryan, F. (1986). High-latitude salinity effects and interhemispheric thermohaline circulations. *Nature 323*, 301–304.

Chamberlin, T. C. (1906). On a possible reversal of deep-sea circulation and its influence on geologic climates. *J. Geology 14*, 363–373.

Chappellaz, J., T. Blunier, D. Raynaud, J. M. Barnola, J. Schwander, & B. Stauffer (1993). Synchronous changes in atmospheric CH_4 and Greenland climate between 40 and 8 kyr BP. *Nature 366*, 443–445.

Crowley, T. J. (1992). North Atlantic deep water cools the southern hemisphere. *Paleoceanogr. 7*, 489–497.

Crowley, T. J. & S. K. Baum (1997). Effect of vegetation on an ice-age climate model simulation. *J. Geophys. Res. 102*, 16463–16480.

Crowley, T. J. & G. R. North (1991). *Paleoclimatology*. Number 18 in Oxford Monographs on Geology and Geophysics. Oxford University Press. 339 pp.

Dansgaard, W., S. J. Johnsen, H. B. Clausen, D. Dahl-Jensen, N. S. Gundestrup, C. U. Hammer, C. S. Hvidberg, J. P. Steffensen, A. E. Sveinbjornsdottir, J. Jouzel, & G. Bond (1993). Evidence for general instability of past climate from a 250-kyr ice-core record. *Nature 364*, 218–220.

Dixon, K. W., T. L. Delworth, M. J. Spelman, & R. J. Stouffer (1999). The influence of transient surface fluxes on North Atlantic overturning in a coupled GCM climate change experiment. *Geophys. Res. Let. 26*, 2749–2752.

Fanning, A. F. & A. J. Weaver (1997). Temporal-geographical meltwater influences on the North Atlantic conveyor: implications for the Younger Dryas. *Paleoceanogr. 12*, 307–320.

Fischer, H., M. Wahlen, J. Smith, D. Mastroianni, & B. Deck (1999). Ice core records of atmospheric CO_2 around the last three glacial terminations. *Science 283*, 1712–1714.

Flückiger, J., A. Dällenbach, T. Blunier, B. Stauffer, T. F. Stocker, D. Raynaud, & J.-M. Barnola (1999). Variations in atmospheric N_2O concentration during abrupt climatic changes. *Science 285*, 227–230.

Fronval, T., E. Jansen, J. Bloemendal, & S. Johnsen (1995). Oceanic evidence for coherent fluctuations in Fennoscandian and Laurentide ice sheets on millennium timescales. *Nature 374*, 443–446.

Gordon, A. L. (1986). Interocean exchange of thermocline water. *J. Geophys. Res. 91*, 5037–5046.

Grimm, E. C., G. L. Jacobson Jr., W. A. Watts, B. C. S. Hanson, & K. A. Maasch (1993). A 50,000-year record of climate oscillations from Florida and its temporal correlation with the Heinrich events. *Science 261*, 198–200.

Gwiazda, R. H., S. R. Hemming, & W. S. Broecker (1996). Provenance of icebergs during Heinrich event 3 and the contrast to their sources during other Heinrich episodes. *Paleoceanogr. 11*, 371–378.

Hall, M. M. & H. L. Bryden (1982). Direct estimates and mechanisms of ocean heat transport. *Deep Sea Res. 29*, 339–359.

Heinrich, H. (1988). Origin and consequences of cyclic ice rafting in the Northeast Atlantic Ocean during the past 130,000 years. *Quat. Res. 29*, 142–152.

Hughen, K. A., J. T. Overpeck, L. C. Peterson, & S. Trumbore (1996). Rapid climate changes in the tropical Atlantic region during the last deglaciation. *Nature 380*, 51–54.

Hughes, T. M. C. & A. J. Weaver (1994). Multiple equilibria of an asymmetric two-basin ocean model. *J. Phys. Oceanogr. 24*, 619–637.

Indermühle, A., E. Monnin, B. Stauffer, T. F. Stocker, & M. Wahlen (2000). Atmospheric CO_2 concentration from 60 to 20 kyr BP from the Taylor Dome ice core, Antarctica. *Geophys. Res. Let. 27*, 735–738.

Indermühle, A., T. F. Stocker, F. Joos, H. Fischer, H. J. Smith, M. Wahlen, B. Deck, M. D., J. Tschumi, T. Blunier, R. Meyer, & B. Stauffer (1999). Holocene carbon-cycle dynamics based on CO_2 trapped in ice at Taylor Dome, Antarctica. *Nature 398*, 121–126.

Johnsen, S. J., D. Dahl-Jensen, W. Dansgaard, & N. Gundestrup (1995). Greenland palaeotemperatures derived from GRIP bore hole temperature and ice core isotope profiles. *Tellus 47B*, 624–629.

Joos, F., R. Meyer, M. Bruno, & M. Leuenberger (1999). The variability in the carbon sinks as reconstructed for the last 1000 years. *Geophys. Res. Let. 26*, 1437–1440.

Joos, F., G.-K. Plattner, T. F. Stocker, O. Marchal, & A. Schmittner (1999). Global warming and marine carbon cycle feedbacks on future atmospheric CO_2. *Science 284*, 464–467.

Joos, F. & J. L. Sarmiento (1995). Der atmosphärische CO_2-Anstieg. *Physikal. Blätter 51*, 405–411.

Keeling, C. D. & T. P. Whorf (1994). Atmospheric CO_2 records from sites in the SIO network. In T. Boden, D. Kaiser, R. Sepanski, & F. Stoss (Eds.), *Trends '93: A Compendium of Data on Global Change*, pp. 16–26. Carbon Dioxide Information Analysis Center.

Killworth, P. D. (1983). Deep convection in the world ocean. *Rev. Geophys. Space Phys. 21*, 1–26.

Knutti, R., T. F. Stocker, & D. G. Wright (2000). The effects of sub-grid-scale parameterizations in a zonally averaged ocean model. *J. Phys. Oceanogr. 30*, 2738–2752.

Lang, C., M. Leuenberger, J. Schwander, & S. Johnsen (1999). 16°C rapid temperature variation in Central Greenland 70,000 years ago. *Science 286*, 934–937.

Macdonald, A. M. & C. Wunsch (1996). An estimate of global ocean circulation and heat fluxes. *Nature 382*, 436–439.

Maier-Reimer, E., U. Mikolajewicz, & A. Winguth (1996). Future ocean uptake of CO_2: interaction between ocean circulation and biology. *Clim. Dyn. 12*, 711–721.

Manabe, S. & R. J. Stouffer (1988). Two stable equilibria of a coupled ocean-atmosphere model. *J. Clim. 1*, 841–866.

Manabe, S. & R. J. Stouffer (1993). Century-scale effects of increased atmospheric CO_2 on the ocean-atmosphere system. *Nature 364*, 215–218.

Manabe, S. & R. J. Stouffer (1994). Multiple-century response of a coupled ocean–atmosphere model to an increase of atmospheric carbon dioxide. *J. Clim. 7*, 5–23.

Marchal, O., T. F. Stocker, & F. Joos (1998). Impact of oceanic reorganizations on the ocean carbon cycle and atmospheric carbon dioxide content. *Paleoceanogr. 13*, 225–244.

Marchal, O., T. F. Stocker, F. Joos, A. Indermühle, T. Blunier, & J. Tschumi (1999). Modelling the concentration of atmospheric CO_2 during the Younger Dryas climate event. *Clim. Dyn. 15*, 341–354.

Marotzke, J., P. Welander, & J. Willebrand (1988). Instability and multiple equilibria in a meridional-plane model of the thermohaline circulation. *Tellus 40A*, 162–172.

Marotzke, J. & J. Willebrand (1991). Multiple equilibria of the global thermohaline circulation. *J. Phys. Oceanogr. 21*, 1372–1385.

Marshall, J. & F. Schott (1999). Open-ocean convection: observations, theory and models. *Rev. Geophys. 37*, 1–64.

Martin, J. H. (1990). Glacial-interglacial CO_2 change: the iron hypothesis. *Paleoceanogr. 5*, 1–13.

McCabe, A. M. & P. U. Clark (1998). Ice-sheet variability around the North Atlantic Ocean during the last deglaciation. *Nature 392*, 373–377.

Mikolajewicz, U. & E. Maier-Reimer (1994). Mixed boundary conditions in ocean general circulation models and their influence on the stability of the model's conveyor belt. *J. Geophys. Res. 99*, 22633–22644.

Neftel, A., E. Moor, H. Oeschger, & B. Stauffer (1985). Evidence from polar ice cores for the increase in atmospheric CO_2 in the past two centuries. *Nature 315*, 45–47.

Neftel, A., H. Oeschger, T. Staffelbach, & B. Stauffer (1988). CO_2 record in the Byrd ice core 50,000–5,000 years BP. *Nature 331*, 609–611.

Pedlosky, J. (1996). *Ocean Circulation Theory*. Springer. 453 pp.

Peixoto, J. P. & A. H. Oort (1992). *Physics of Climate*. American Institute of Physics. 500 pp.

Petit, J. R., J. Jouzel, D. Raynaud, N. I. Barkov, J.-M. Barnola, I. Basile, M. Bender, J. Chappellaz, M. Davis, G. Delaygue, M. Delmotte, V. M. Kotlyakov, M. Legrand, V. Y. Lipenkov, C. Lorius, L. Pépin, C. Ritz, E. Saltzman, & M. Stievenard (1999). Climate and atmospheric history of the past 420,000 years from the Vostok ice core, Antarctica. *Nature 399*, 429–436.

Rahmstorf, S. & J. Willebrand (1995). The role of temperature feedback in stabilizing the thermohaline circulation. *J. Phys. Oceanogr. 25*, 787–805.

Raynaud, D., J. Jouzel, J. M. Barnola, J. Chappellaz, R. J. Delmas, & C. Lorius (1993). The ice record of greenhouse gases. *Science 259*, 926–934.

Rooth, C. (1982). Hydrology and ocean circulation. *Prog. Oceanogr. 11*, 131–149.

Sarmiento, J. L. & C. Le Quéré (1996). Oceanic carbon dioxide in a model of century-scale global warming. *Science 274*, 1346–1350.

Schiller, A., U. Mikolajewicz, & R. Voss (1997). The stability of the North Atlantic thermohaline circulation in a coupled ocean-atmosphere general circulation model. *Clim. Dyn. 13*, 325–347.

Schmittner, A. & T. F. Stocker (1999). The stability of the thermohaline circulation in global warming experiments. *J. Clim. 12*, 1117–1133.

Schmitz, W. J. (1995). On the interbasin-scale thermohaline circulation. *Rev. Geophys. 33*, 151–173.

Schwander, J., T. Sowers, J.-M. Barnola, T. Blunier, A. Fuchs, & B. Malaizé (1997). Age scale of the air in the Summit ice: Implication for glacial-interglacial temperature change. *J. Geophys. Res. 102*, 19483–19493.

Severinghaus, J. P., T. Sowers, E. J. Brook, R. B. Alley, & M. L. Bender (1998). Timing of abrupt climate change at the end of the Younger Dryas interval from thermally fractionated gases in polar ice. *Nature 391*, 141–146.

Siegenthaler, U. & J. L. Sarmiento (1993). Atmospheric carbon dioxide and the ocean. *Nature 365*, 119–125.

Siegenthaler, U. & T. Wenk (1984). Rapid atmospheric CO_2 variations and ocean circulation. *Nature 308*, 624–626.

Stauffer, B., T. Blunier, A. Dällenbach, A. Indermühle, J. Schwander, T. F. Stocker, J. Tschumi, J. Chappellaz, D. Raynaud, C. U. Hammer, & H. B. Clausen (1998). Atmospheric CO_2 and millennial-scale climate change during the last glacial period. *Nature 392*, 59–62.

Stocker, T. F. (1998). The seesaw effect. *Science 282*, 61–62.

Stocker, T. F. (1999). Climate changes: from the past to the future – a review. *Int. J. Earth Sci. 88*, 365–374.

Stocker, T. F. (2000). Past and future reorganisations in the climate system. *Quat. Sci. Rev. 19*, 301–319.

Stocker, T. F. & A. Schmittner (1997). Influence of CO_2 emission rates on the stability of the thermohaline circulation. *Nature 388*, 862–865.

Stocker, T. F. & D. G. Wright (1991). Rapid transitions of the ocean's deep circulation induced by changes in surface water fluxes. *Nature 351*, 729–732.

Stommel, H. (1948). The westward intensification of wind-driven ocean currents. *Trans. Am. Geophys. Union 29*, 202–206.

Stommel, H. (1958). The abyssal circulation. *Deep Sea Res. 5*, 80–82.

Stommel, H. (1961). Thermohaline convection with two stable regimes of flow. *Tellus 13*, 224–241.

Stommel, H. & A. B. Arons (1960). On the abyssal circulation of the world ocean - I. Stationary planetary flow patterns on a sphere. *Deep Sea Res. 6*, 140–154.

Takahashi, T., J. Olafsson, J. G. Goddard, D. W. Chipman, & S. C. Sutherland (1993). Seasonal variation of CO_2 and nutrients in the high-latitude surface oceans: a comparative study. *Global Biogeochem. Cyc. 7*, 843–878.

Trenberth, K. E. & A. Solomon (1994). The global heat balance: heat transports in the atmosphere and ocean. *Clim. Dyn. 10*, 107–134.

Volk, T. & M. I. Hoffert (1985). Ocean carbon pumps: analysis of relative strengths and efficiencies in ocean-driven atmospheric CO_2 changes. In E. T. Sundquist & W. S. Broecker (Eds.), *The Carbon Cycle and Atmospheric CO_2: Natural Variations Archean to Present*, Volume 32 of *Geophysical Monograph*, pp. 99–110. Am. Geophys. Union.

Warren, B. A. (1981). Deep circulation of the world ocean. In B. A. Warren & C. Wunsch (Eds.), *Evolution of Physical Oceanography – Scientific Surveys in Honor of Henry Stommel*, pp. 6–41. MIT Press.

Wood, R. A., A. B. Keen, J. F. B. Mitchell, & J. M. Gregory (1999). Changing spatial structure of the thermohaline circulation in response to atmospheric CO_2 forcing in a climate model. *Nature 399*, 572–575.

Wright, D. G. & T. F. Stocker (1991). A zonally averaged ocean model for the thermohaline circulation, Part I: Model development and flow dynamics. *J. Phys. Oceanogr. 21*, 1713–1724.